

# Evidence of Preorganization in Quinonoid Intermediate Formation from L-Trp in H463F Mutant *Escherichia coli* Tryptophan Indole-lyase from Effects of Pressure and pH

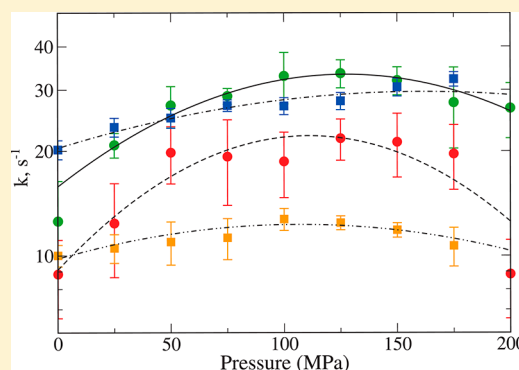
Robert S. Phillips,<sup>\*,†</sup> Ukoha Kalu,<sup>†</sup> and Sam Hay<sup>‡</sup>

<sup>†</sup>Department of Chemistry and Department of Biochemistry and Molecular Biology, University of Georgia, Athens, Georgia 30602, United States

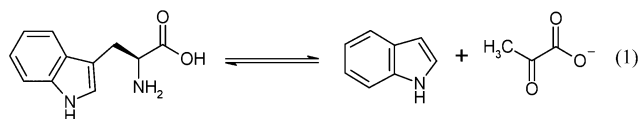
<sup>‡</sup>Manchester Interdisciplinary Biocentre and Faculty of Life Sciences, University of Manchester, 131 Princess Street, Manchester M1 7DN, U.K.

**ABSTRACT:** The effects of pH and hydrostatic pressure on the reaction of H463F tryptophan indole-lyase (TIL) have been evaluated. The mutant TIL shows very low activity for elimination of indole but is still competent to form a quinonoid intermediate from L-tryptophan [Phillips, R. S., Johnson, N., and Kamath, A. V. (2002) *Biochemistry* 41, 4012–4019]. Stopped-flow measurements show that the formation of the quinonoid intermediate at 505 nm is affected by pH, with a bell-shaped dependence for the forward rate constant,  $k_f$ , and dependence on a single basic group for the reverse rate constant,  $k_r$ , with the following values:  $pK_{a1} = 8.14 \pm 0.15$ ,  $pK_{a2} = 7.54 \pm 0.15$ ,  $k_{f,min} = 18.1 \pm 1.3 \text{ s}^{-1}$ ,  $k_{f,max} = 179 \pm 46.3 \text{ s}^{-1}$ ,  $k_{r,min} = 11.4 \pm 1.2 \text{ s}^{-1}$ , and  $k_{r,max} = 33 \pm 1.6 \text{ s}^{-1}$ . The pH effects may be due to ionization of Tyr74 as the base and Cys298 as the acid influencing the rate constant for deprotonation. High-pressure stopped-flow measurements were performed at pH 8, which is the optimum for the forward reaction.

The rate constants show an increase with pressure up to 100 MPa and a subsequent decrease above 100 MPa. Fitting the pressure data gives the following values:  $k_{f,0} = 15.4 \pm 0.8 \text{ s}^{-1}$ ,  $\Delta V^\ddagger = -29.4 \pm 2.9 \text{ cm}^3 \text{ mol}^{-1}$ , and  $\Delta\beta^\ddagger = -0.23 \pm 0.03 \text{ cm}^3 \text{ mol}^{-1} \text{ MPa}^{-1}$  for the forward reaction, and  $k_{r,0} = 20.7 \pm 0.8 \text{ s}^{-1}$ ,  $\Delta V^\ddagger = -9.6 \pm 2.3 \text{ cm}^3 \text{ mol}^{-1}$ , and  $\Delta\beta^\ddagger = -0.05 \pm 0.02 \text{ cm}^3 \text{ mol}^{-1} \text{ MPa}^{-1}$  for the reverse reaction. The primary kinetic isotope effect on quinonoid intermediate formation at pH 8 is small ( $\sim 2$ ) and is not significantly pressure-dependent, suggesting that the effect of pressure on  $k_f$  may be due to perturbation of an active site preorganization step. The negative activation volume is also consistent with preorganization of the ES complex prior to quinonoid intermediate formation, and the negative compressibility may be due to the effect of pressure on the enzyme conformation. These results support the conclusion that the preorganization of the H463F TIL Trp complex, which is probably dominated by motion of the L-Trp indole moiety of the aldimine complex, contributes to quinonoid intermediate formation.



**T**ryptophan indole-lyase (TIL, tryptophanase, EC 4.1.99.1) is a pyridoxal 5'-phosphate (PLP) enzyme that catalyzes the reversible hydrolytic  $\beta$ -elimination of L-tryptophan to give indole and ammonium pyruvate (eq 1). This enzyme is widely



distributed in enterobacteria, particularly in *Escherichia coli*.<sup>1</sup> Although indole was long considered to be simply a waste product of bacterial metabolism of L-Trp, recently it has been discovered that indole is a bacterial signaling molecule that regulates gene expression,<sup>2</sup> biofilm formation,<sup>3–5</sup> plasmid stability,<sup>6</sup> pathogenicity,<sup>7</sup> and antibiotic resistance.<sup>8</sup> Thus, because TIL is not found in eukaryotes, the enzyme is a potential target for novel selective antibacterial drugs.

The mechanism of indole elimination catalyzed by TIL is intriguing, because indole is a poor leaving group for a conventional  $\beta$ -elimination. The proposed mechanism involves the initial formation of an external aldimine with the PLP, followed by  $\alpha$ -deprotonation to give a quinonoid intermediate (Scheme 1).<sup>9–11</sup> Subsequently, the transfer of a proton to the indole C<sub>3</sub> occurs, followed by or concerted with, elimination with C <sub>$\beta$</sub> –C<sub>3</sub> bond cleavage.<sup>11</sup> In previous studies, we examined the H463F mutant TIL, which was designed to evaluate whether His463 formed a hydrogen bond to the indole NH of the Trp substrate. This mutant enzyme has very low activity for indole elimination (step 4 in Scheme 1) but still can efficiently form a quinonoid intermediate,<sup>12</sup> which becomes kinetically trapped. Therefore, H463F TIL is useful in the study of the TIL mechanism up to formation of the quinonoid complex (steps

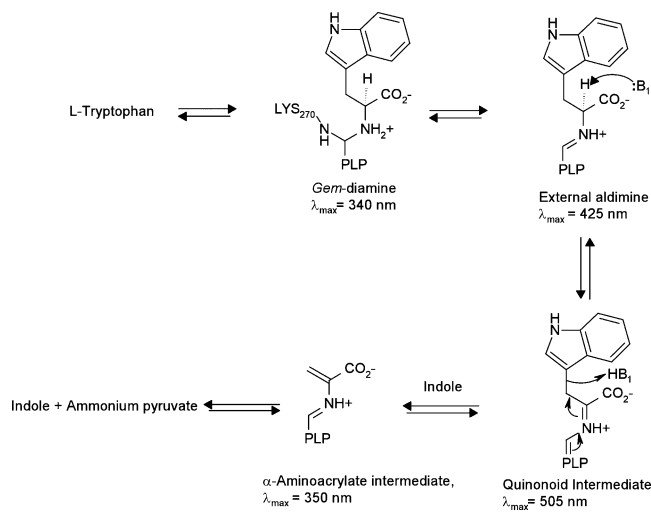
**Received:** May 15, 2012

**Revised:** July 13, 2012

**Published:** August 1, 2012



Scheme 1. Mechanism of TIL



1–3 in Scheme 1). In subsequent pressure-jump (*p*-jump) experiments, we found that the rate constant of quinonoid intermediate formation from L-Trp, but not L-Met, with H463F TIL increased with pressure up to 40 MPa (400 bar; 1 bar = 0.987 atm),<sup>13</sup> the upper pressure limit of the pressure-jump instrument. As this differential pressure response may be of mechanistic origin, we have now used stopped-flow spectrophotometry, which has a much larger experimental pressure range (200 cf. 40 MPa), to further examine the effects of pH and pressure on formation of the H463F-L-Trp quinonoid intermediate from L-Trp and α-[<sup>2</sup>H]-L-Trp. The results of these experiments are presented herein.

## EXPERIMENTAL PROCEDURES

**Materials.** L-Tryptophan was a product of US Biochemicals. Triethanolamine and other laboratory reagents were obtained from Fisher Scientific. All enzyme solutions were prepared in deionized distilled water.

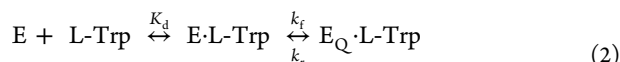
**Enzyme.** H463F mutant TIL was prepared as described previously.<sup>12</sup> The protein concentration was determined from the absorbance at 280 nm [*A*<sub>280</sub>(1%) = 9.19]<sup>14</sup> or using the Bio-Rad Bradford protein dye reagent<sup>15</sup> with wild-type TIL as a standard. The enzyme activity was measured with *S*-(*o*-nitrophenyl)-L-Cys,<sup>16</sup> which is less sensitive than L-Trp to the effects of mutation in the active site.

**α-[<sup>2</sup>H]-L-Tryptophan.** L-Tryptophan (0.162 g) was dissolved in 20 mL of <sup>2</sup>H<sub>2</sub>O, and 0.4 mL of H463F TIL (16 mg/mL) in aqueous phosphate buffer was added. The reaction mixture was left at room temperature for 7 days, at which time <sup>1</sup>H NMR showed the α-proton was >95% exchanged. The reaction mixture was applied to a column (1.5 cm × 10 cm) of Dowex-50 (H<sup>+</sup>); the column was washed with water until the washings were neutral, and the amino acid was eluted with 1 M NH<sub>3</sub>. The eluate (30 mL) was evaporated in vacuo, and the solid residue was suspended in 95% ethanol and filtered, giving 0.12 g of cream-colored powder.

**Instruments.** Atmospheric-pressure stopped-flow experiments were performed at ambient temperature (~22–23 °C) with an Applied Photophysics SX.18MV-R stopped-flow spectrophotometer in single-wavelength mode at 505 nm. The pressure-dependent stopped-flow experiments were performed at 20 °C in a HiTech HP-SF Scientific stopped-flow spectrophotometer (TgK Scientific, Bradford on Avon,

U.K.). The protein was exchanged into 0.1 M triethanolamine hydrochloride (pH 8.0) and 0.1 M KCl, with a PD-10 gel filtration column before the experiments. This buffer was used because triethanolamine has a low Δ*pK*<sub>a</sub> value with pressure (Δ*V*<sup>‡</sup> = 4.5 ± 0.3<sup>17</sup>), minimizing any possible change in pH with pressure. For pH dependence, the buffer consisted of 0.1 M triethanolamine phosphate and 0.1 M KCl, adjusted to the desired nominal pH from 6.5 to 9.0 in 0.5 pH unit steps. The enzyme was exchanged with a PD-10 gel filtration column equilibrated with the various buffers immediately prior to the experiments. The actual pH of the buffer after dilution was measured to plot the results in Figure 3.

**Data Analysis.** The concentration dependence of the stopped-flow data was fit to eq 3, assuming the kinetic model shown in eq 2



$$k_{\text{obs}} = k_f[L\text{-Trp}]/(K_d + [L\text{-Trp}]) + k_r \quad (3)$$

where *k*<sub>obs</sub> is the rate constant at any L-Trp concentration, *k*<sub>f</sub> is the rate constant for the forward reaction (α-deprotonation), *K*<sub>d</sub> is the dissociation constant for L-Trp, and *k*<sub>r</sub> is the rate constant for the reverse reaction (α-protonation). The pH dependence data were fit to eq 4 for a bell-shaped pH profile with a limiting minimum value, *k*<sub>min</sub>.

$$k_{\text{obs}} = k_{\text{max}}/(1 + 10^{-\text{pH}}/10^{-\text{pK}_{a1}} + 10^{-\text{pK}_{a2}}/10^{-\text{pH}}) + k_{\text{min}} \quad (4)$$

Global fitting was performed with a shared *pK*<sub>a,1</sub> value using Origin 8.1 (OriginLab). The pressure dependence data were fit to eq 5

$$k_{\text{obs}} = k_o \exp(-\Delta V^\ddagger p/RT) \exp(\Delta\beta^\ddagger p^2/2RT) \quad (5)$$

where Δ*V*<sup>‡</sup> is the activation volume, Δ*β*<sup>‡</sup> is the transition state compressibility, and *R* is the ideal gas constant (8.314 cm<sup>3</sup> MPa mol<sup>−1</sup> K<sup>−1</sup>).

**Modeling.** Density function theory (DFT) calculations of the external aldimine and quinonoid intermediates were performed using B3LYP/6-31G(d) with Gaussian 03 revision D.<sup>18</sup> The two models containing the relevant PLP, truncated by removing the PO<sub>4</sub><sup>2−</sup> moiety, and the Trp moieties were geometry optimized in the gas phase. All models were aligned over the six PLP ring atoms.

## RESULTS AND DISCUSSION

**pH Dependence of L-Trp Quinonoid Complex Formation.** While the rate of turnover of the H463F mutant TIL is much lower than the wild-type rate,<sup>12</sup> this enzyme readily reacts with L-Trp at pH 8 to form a quinonoid complex, with a λ<sub>max</sub> at 505 nm, that is similar to wild-type TIL (Figure 1A). This quinonoid complex is kinetically trapped because of the relatively rapid α-deprotonation reaction, together with the very slow elimination (steps 1–3 and 4, respectively, in Scheme 1). Fitting the stopped-flow data for the first 200 ms of the reaction to a single exponential gives a reasonable fit (Figure 1B). The apparent rate constant for quinonoid intermediate formation, *k*<sub>obs</sub>, exhibits a hyperbolic dependence on L-Trp concentration (Figure 2), indicating that there is a rapid binding equilibrium, followed by a slower step in which the quinonoid species is formed (eq 2). Fitting the concentration dependence data in Figure 2 to eq 3 provides the apparent rate constants at pH 8 for deprotonation (*k*<sub>f</sub> = 49.4 ± 2.4 s<sup>−1</sup>) and reprotonation (*k*<sub>r</sub> =

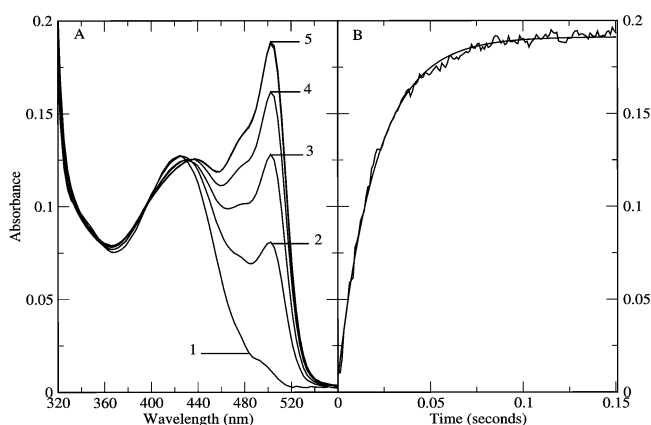


**Figure 1.** Spectroscopic changes during the reaction of H463F TIL with L-Trp. (A) Reaction of H463F TIL (1 mg/mL) in 0.05 M potassium phosphate (pH 8.0) with 20 mM L-Trp. Scans are shown at 0.3, 10.3, 20.3, 40.3, and 80.3 ms (1–5, respectively). (B) The time course at 504 nm fit to a single-exponential function.

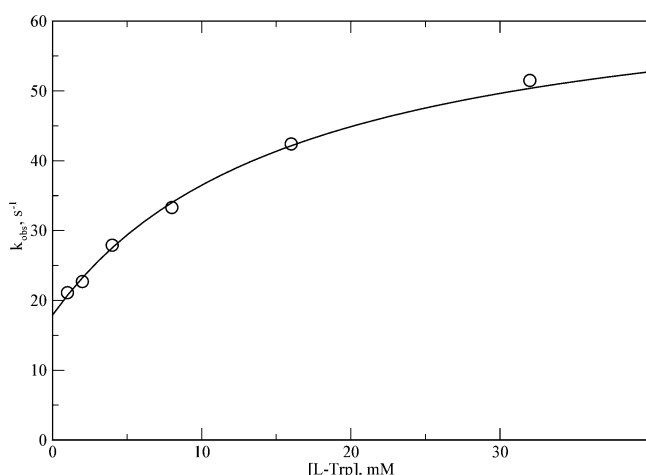


**Figure 2.** Concentration dependence of quinonoid intermediate formation. The reactions were performed with H463F TIL (1 mg/mL) in 0.1 M triethanolamine phosphate (pH 8.0) and 0.1 M KCl. The line is the result of fitting the data to eq 3.

$17.9 \pm 1.0 \text{ s}^{-1}$ ). These constants are  $\sim 1$  order of magnitude slower than what is seen for quinonoid intermediate formation from L-Trp with wild-type TIL.<sup>9–11</sup> The concentration-dependent stopped-flow measurements like that shown in Figure 2 were also performed at pH values ranging from 6.5 to 9.5, and the rate constants found after fitting are pH-dependent, with the results shown in Figure 3. Fitting the data in Figure 3 for both  $k_f$  and  $k_r$  simultaneously to eq 4 gives the following values:  $\text{pK}_{a1} = 8.14 \pm 0.15$ ,  $\text{pK}_{a2} = 7.54 \pm 0.15$ ,  $k_{f,\text{min}} = 18.1 \pm 1.3 \text{ s}^{-1}$ ,  $k_{f,\text{max}} = 179 \pm 46.3 \text{ s}^{-1}$ ,  $k_{r,\text{min}} = 11.4 \pm 1.2 \text{ s}^{-1}$ , and  $k_{r,\text{max}} = 33 \pm 1.6 \text{ s}^{-1}$ . The lines in Figure 3 are the fitted curves using these parameters. Because the rate constant does not decrease logarithmically at high and low pH but rather reaches a minimum, the acid with a  $\text{pK}_a$  of 8.14 and the base with a  $\text{pK}_a$  of 7.54 are not the groups directly involved in the deprotonation but rather must be auxiliaries whose ionization states modulate the enzyme reactivity, perhaps by affecting the enzyme conformation. The deprotonation is influenced by both the acidic and basic ionizations, but the reprotonation is influenced by only the base. It is interesting in this regard that the PLP spectrum of wild-type TIL exhibits pH-dependent

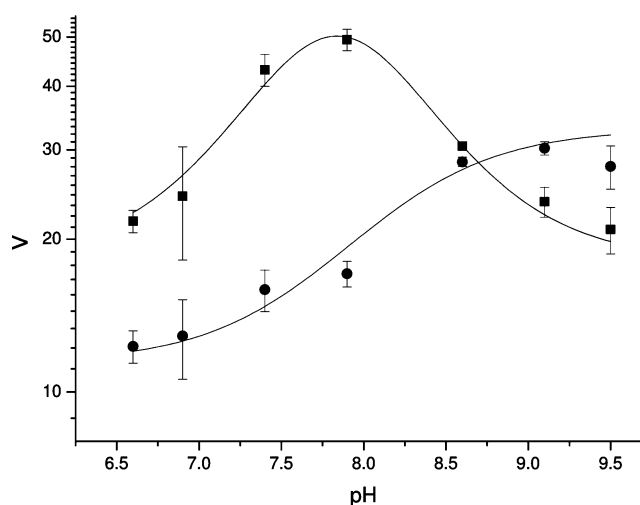


**Figure 3.** pH dependence of quinonoid intermediate formation:  $k_f$  (●) and  $k_r$  (■). The reactions were performed as shown in Figure 2, in 0.1 M triethanolamine phosphate and 0.1 M KCl, at pH values ranging from 6.5 to 9.5. The lines are the curves from fitting the data to eq 4.

interconversion of ketoenamine and enolimine tautomers, absorbing at 423 and 338 nm, respectively, showing a  $\text{pK}_a$  of 7.5–7.8.<sup>14,19,20</sup> Thus, the acidic group observed in these experiments with a  $\text{pK}_a$  of 8.14 is possibly Cys298, because mutation of this Cys residue in the active site to Ser affects the PLP spectrum and the pH dependence of the reaction<sup>14</sup> (Scheme 2). The basic group with a  $\text{pK}_a$  of 7.54 may be the tyrosinate form of Tyr-74, which is likely to be the proton donor to the leaving group for the elimination (Scheme 2), because Y74F mutant TIL exhibits no detectable elimination activity with L-Trp but retains activity with other substrates with good leaving groups.<sup>12</sup> Furthermore, the crystal structures of the paralogous tyrosine phenol-lyase (TPL) F448H mutant with 3-F-Tyr bound show that Tyr71, homologous with Tyr74 in TIL, is located near the  $\gamma$ -carbon of the substrate and forms a hydrogen bond to the active site Lys257 in the quinonoid complex. Although the  $\text{pK}_a$  of the phenol of free tyrosine in solution is 10.1, an active site tyrosine with a  $\text{pK}_a = 7.5$  is not unprecedented. As an example, it has been shown in alanine racemase that a tyrosinate is a catalytic base, with a  $\text{pK}_a$  value of 7.1–7.4.<sup>21</sup>

**Pressure Dependence of L-Trp Quinonoid Complex Formation.** Previous *p*-jump kinetic measurements of the reaction of H463F TIL with L-Trp at pressures of up to 40 MPa found that the reaction showed a significant increase in rate constant under pressure.<sup>13</sup> However, we were unable to perform *p*-jumps at higher pressures because of instrumental limitations. Hence, we were interested in using high-pressure stopped-flow spectrophotometry to obtain kinetic data at higher pressures. Because the rate constant and amplitude at 505 nm of quinonoid intermediate formation are optimal at pH 8 (Figure 3), the subsequent pressure-dependent stopped-flow kinetics experiments were performed at pH 8 and 293 K. The pressure dependence was performed at 1.75 and 19 mM L-Trp, as at these concentrations, the observed rate constant,  $k_{\text{obs}}$ , is approximately equal to  $k_r$  and  $k_f + k_r$ , respectively (Figure 2). Thus,  $k_f$  can be approximated by  $k_{\text{obs}}(19 \text{ mM}) - k_{\text{obs}}(1.75 \text{ mM})$ . The observed rate constants were found to increase with pressure, up to a maximum at  $\sim 100 \text{ MPa}$ , and then decrease (Figure 4A). Thus, we fit the pressure-dependent data with a

## Scheme 2. Role of Tyr71 and Cys298 in Quinonoid Intermediate Formation

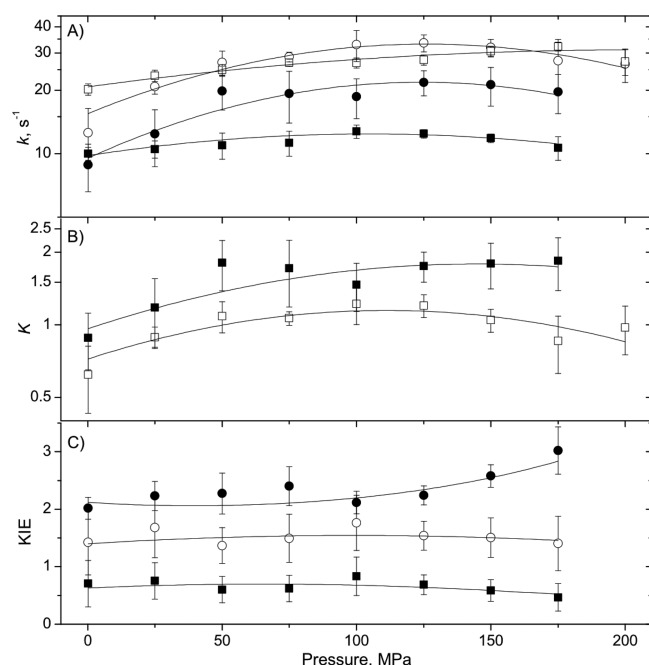
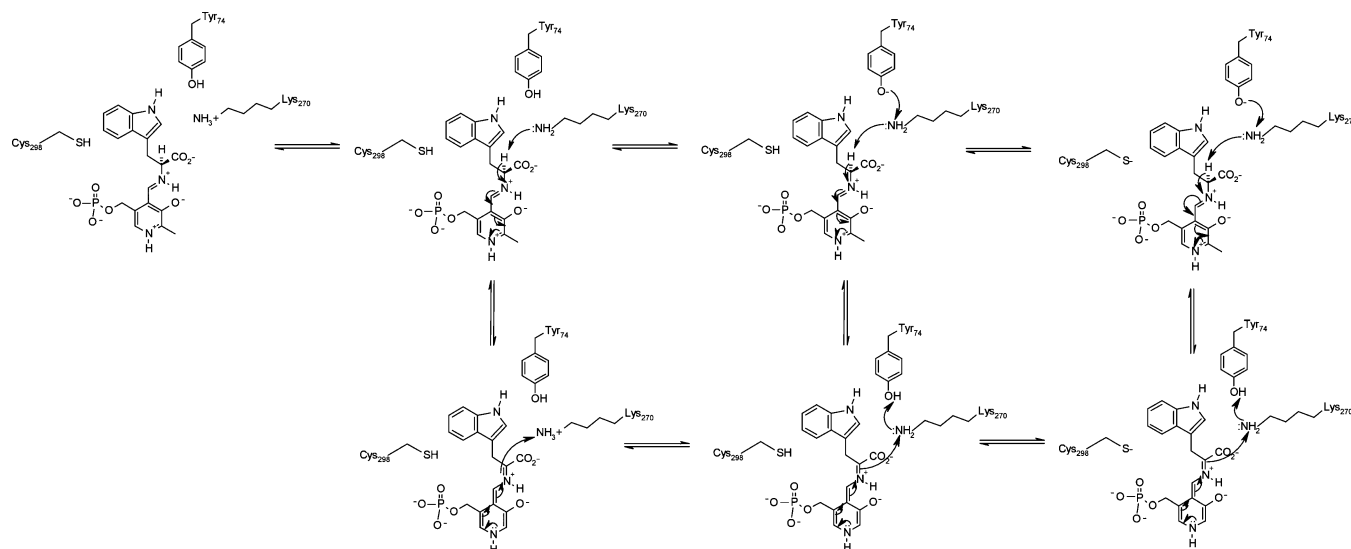


**Figure 4.** Effect of hydrostatic pressure on the reaction of 1 mg/mL *E. coli* H463F mutant TIL with L-Trp and  $\alpha$ - $^2\text{H}$ -L-Trp at 293 K and pH 8.0. (A)  $k_f(\text{H})$  (○),  $k_r(\text{H})$  (□),  $k_f(\text{D})$  (●), and  $k_r(\text{D})$  (■). (B) Equilibrium constant  $K = k_f/k_r$  on H (□) and D (■) transfer. (C) KIEs on  $k_f$  (○),  $k_r$  (●), and  $K$  (■). The data are fit to eq 5, and fitted parameters are listed in Table 1.

nonlinear equation, including both the apparent activation volume ( $\Delta V^\ddagger$ ) and compressibility ( $\Delta\beta^\ddagger$ , eq 5). The results of the fits are shown in Figure 4A, with the parameters listed in Table 1. The initial increase in  $k_f$  with pressure is due to a  $\Delta V^\ddagger$  of  $-29.4 \pm 2.9 \text{ cm}^3 \text{ mol}^{-1}$ , in good agreement with the previous results of *p*-jump experiments in the pressure range of 10–40 MPa, where we obtained a  $\Delta V^\ddagger$  of  $-26.5 \text{ cm}^3 \text{ mol}^{-1}$ .<sup>13</sup> It is interesting that the  $\Delta V^\ddagger$  for  $k_r$  of  $-11.5 \text{ cm}^3 \text{ mol}^{-1}$  is much smaller than for  $k_f$ . Although we have analyzed the data with eq 5 assuming that the increase in the rate constants is due to  $\Delta V^\ddagger$ , it is also possible that the  $\text{pK}_a$  values are pressure-dependent. At pressures of >100 MPa, the decrease in  $k_r$  is the

result of the  $\Delta\beta^\ddagger$  of  $-0.23 \text{ cm}^3 \text{ mol}^{-1} \text{ MPa}^{-1}$ . As was found with  $\Delta V^\ddagger$ ,  $\Delta\beta^\ddagger$  is smaller for  $k_r$  (only  $-0.05 \text{ cm}^3 \text{ mol}^{-1} \text{ MPa}^{-1}$ ). We found previously that the binding of Trp may be affected by pressure,<sup>13</sup> especially at subsaturating concentrations. However, in this work we see a large  $\Delta\beta^\ddagger$  even in the 19 mM experiments, which is not likely to be due to effects on binding.

The equilibrium constant ( $K = k_f/k_r$ ) is 0.72 at 1 bar and increases with pressure, with a  $\Delta V$  of  $-20.4 \text{ cm}^3 \text{ mol}^{-1}$  and a  $\Delta\beta$  of  $-0.18 \pm 0.05 \text{ cm}^3 \text{ mol}^{-1} \text{ MPa}^{-1}$  (Figure 4B and Table 1). In this case, the  $\Delta V$  describes the reduction in the reaction volume between the L-Trp external aldimine and the quinonoid intermediate, while the negative compressibility indicates that the quinonoid intermediate is also less compressible than the L-Trp external aldimine. The smaller volume and reduced compressibility of the quinonoid intermediate are likely due to the formation of a closed (active) conformation of the enzyme, as was recently observed in crystal structures of quinonoid complexes of the paralogous enzyme, TPL, while the aldimines are in more open conformations.<sup>22,23</sup>

To perform KIE experiments, H463F TIL was used to prepare  $\alpha$ - $^2\text{H}$ -L-Trp by exchange with L-Trp in  $\text{D}_2\text{O}$  (see Experimental Procedures). When the stopped-flow reactions were performed with  $\alpha$ - $^2\text{H}$ -L-Trp, small but significant kinetic isotope effects on the rate constants are observed [ $\text{KIE}_f = 1.6 \pm 0.3$ , and  $\text{KIE}_r = 2.1 \pm 0.1$  (Figure 4B and Table 1)]. It is interesting that the KIE is larger for  $k_r$  than for  $k_f$ , which implies a significant amount of internal return of the  $\alpha$ -proton, despite the ease of H–D exchange during extended incubation. While there are significant KIEs on  $k_f$  and  $k_r$  (and on  $K$ ), there are no significant isotope effects on either  $\Delta V^\ddagger$  or  $\Delta\beta^\ddagger$  (Table 1); i.e., the KIEs are not significantly pressure-dependent. Hydrogen transfer reactions involving a significant degree of nuclear quantum mechanical tunnelling (NQMT) (of the transferred H) have been shown to exhibit pressure dependencies of both the observed rate and KIE.<sup>24,25</sup> Conversely, KIEs arising from semiclassical mechanisms (no significant NQMT) are not expected to be pressure-dependent as these KIEs arise from differences in the vibrational frequencies of the transferred atoms, which have been shown to be relatively insensitive to pressures of a few kilobars.<sup>26</sup> While we cannot rule out the involvement of NQMT during enzyme-catalyzed hydrogen transfer on the basis of a lack of a pressure-dependent KIE,<sup>26–28</sup>



Table 1. Apparent Activation Volumes and Compressibilities for  $\alpha$ -Deprotonation of L-Trp by *E. coli* H463F Mutant TIL<sup>a</sup>

	$k_f$	$k_r$	$K = k_f/k_r$
$k_0^H$ (s <sup>-1</sup> )	15.4 ± 0.8	20.7 ± 0.8	0.72 ± 0.06
$k_0^D$ (s <sup>-1</sup> )	9.5 ± 1.0	9.8 ± 0.3	0.96 ± 0.12
KIE <sub>0</sub>	1.6 ± 0.3	2.1 ± 0.1	0.75 ± 0.15
$\Delta V^{\ddagger H}$ (cm <sup>3</sup> mol <sup>-1</sup> )	-29.4 ± 2.9	-9.6 ± 2.3	-20.4 ± 4.3
$\Delta V^{\ddagger D}$ (cm <sup>3</sup> mol <sup>-1</sup> )	-32.6 ± 6.4	-11.1 ± 2.0	-20.9 ± 7.6
$\Delta\Delta V^{\ddagger}$ (cm <sup>3</sup> mol <sup>-1</sup> )	3.2 ± 9.3	1.3 ± 4.3	0.5 ± 11.9
$\Delta\beta^{\ddagger H}$ (cm <sup>3</sup> mol <sup>-1</sup> MPa <sup>-1</sup> )	-0.23 ± 0.03	-0.05 ± 0.02	-0.18 ± 0.04
$\Delta\beta^{\ddagger D}$ (cm <sup>3</sup> mol <sup>-1</sup> MPa <sup>-1</sup> )	-0.26 ± 0.07	-0.11 ± 0.02	-0.14 ± 0.09
$\Delta\Delta\beta^{\ddagger}$ (cm <sup>3</sup> mol <sup>-1</sup> MPa <sup>-1</sup> )	+0.03 ± 0.10	+0.06 ± 0.05	-0.04 ± 0.13

<sup>a</sup>Values were obtained by fitting the data in Figure 4 to eq 5. KIE values were determined as follows:  $\Delta\Delta V^{\ddagger} = \Delta V^{\ddagger H} - \Delta V^{\ddagger D}$ , and  $\Delta\Delta\beta^{\ddagger} = \Delta\beta^{\ddagger H} - \Delta\beta^{\ddagger D}$ .  $K$  values were determined by fitting the data in Figure 4B to eq 5.

the pressure dependence of  $k_f$  and  $k_r$  and the pressure independence of the KIE suggest that either the reaction does not employ significant quantum mechanical tunneling or the effect of pressure on the observed rate constants is due to pressure perturbing a step that is kinetically coupled to, but independent of, the reaction, e.g., active site closure and/or active site preorganization.

**Implications for the Enzyme Mechanism.** The proposed mechanism of TIL is shown in Scheme 1. L-Trp reacts rapidly, within the dead time of the stopped-flow instrument, with the internal aldimine to form an external aldimine. Subsequent deprotonation of the  $\alpha$ -CH of the external aldimine can then occur to form the resonance-stabilized quinonoid carbanion. Elimination of indole had been thought to occur from the quinonoid by initial transfer of a proton to C<sub>3</sub> to give an indolenine species, followed by C <sub>$\beta$</sub> -C<sub>3</sub> bond cleavage. However, multiple-isotope effect experiments suggest that the proton transfer to C<sub>3</sub> and C <sub>$\beta$</sub> -C<sub>3</sub> bond cleavage may be concerted.<sup>11</sup> H463F TIL has very low elimination activity (<0.1% of that of wild-type TIL) because His463 has been proposed to interact with the substrate indole NH as a base or by hydrogen bonding to facilitate the transfer of a proton to C<sub>3</sub>.<sup>12</sup> However, on the basis of the recent structures of the paralogous enzyme, TPL, that show substrate strain,<sup>21</sup> it is possible that His463 forms a hydrogen bond with the substrate NH to introduce strain that is necessary for efficient catalysis. His463 is obviously not required for quinonoid intermediate formation (Figure 1), although the rate constant is reduced in H463F by ~1 order of magnitude compared with that of wild-type TIL.<sup>12</sup> Thus, it is possible that preorganization of the enzyme-substrate complex contributes to quinonoid intermediate formation. The stereochemical course of the elimination of indole is most likely *anti*, as was found in the quinonoid structures of Y71F and F448H mutant TPL with 3-fluoro-L-tyrosine,<sup>22</sup> so the indole ring must be situated with the C <sub>$\beta$</sub> -C<sub>3</sub> bond antiperiplanar to the  $\alpha$ -C-H bond when deprotonation occurs. In addition, the indole ring should be oriented approximately perpendicular relative to the C <sub>$\alpha$</sub> -C <sub>$\beta$</sub>  bond axis for elimination. Finally, the  $\beta$ -carbon will be moving into the plane of the PLP  $\pi$ -system during quinonoid intermediate formation, and the indole ring will be in motion during deprotonation (Figure 5A). Thus, the positioning of the indole ring into the correct geometry for the elimination to occur will lower the activation energy barrier for quinonoid intermediate formation by reducing the required level of motion. Two stable conformations of both the external aldimine and quinonoid structures were found, and both external aldimine conformers are compared in Figure 5B. Only

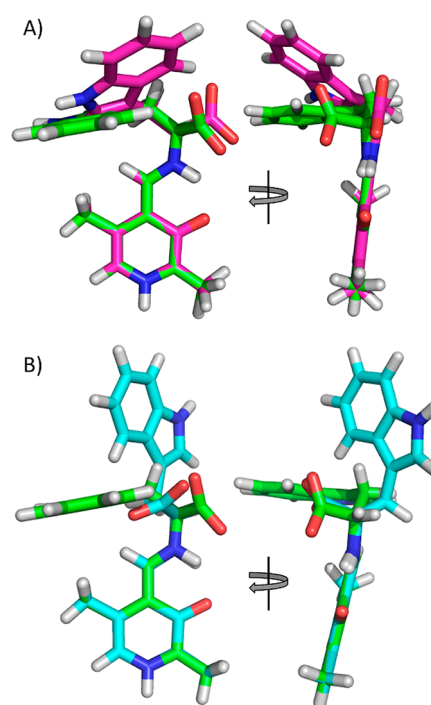


**Figure 5.** Active site preorganization. Orthogonal projections of models of (A) compact conformers of the aldimine intermediate (green carbons) and quinonoid intermediate (magenta carbons) and (B) comparison of the compact and extended conformers of the aldimine intermediate.

the compact quinonoid conformer is compatible with subsequent proton transfer, which has been proposed to occur to the *re*-face of the indole group.<sup>29</sup> Pressure could enhance the rate of reaction in a number of ways. By straining the external aldimine intermediate to form a more quinonoid-like geometry, e.g., by pulling the carboxylate into the plane of the PLP, or by increasing the angle between the PLP and indole rings (Figure 5A), we can enhance the reaction rate due to ground state destabilization. Alternatively, as the external aldimine may adopt multiple conformational states (Figure 5B), if pressure favors the more reactive conformer (in this case, the “compact” form), then the observed rate of reaction will increase with pressure. In this case, the rate enhancement occurs because of preorganization of the reactant state, rather than through direct perturbation of the chemical step. This preorganization of the enzyme-substrate complex results in a negative activation volume and, thus, the observed increase in rate constant with increasing pressure up to ~100 MPa. In

contrast, a competitive inhibitor, L-Met, was found in previous experiments to show no change in rate constant for quinonoid intermediate formation with pressures of up to 40 MPa with either wild-type or H463F TIL,<sup>13</sup> indicating that preorganization is not significant in this case. However, as the proposed preorganization is dominated by movement of the L-Trp indole moiety (Figure 5), the lack of preorganization of L-Met is not unexpected as the S-CH<sub>3</sub> moiety of L-Met is much smaller than the L-Trp indole. Together, these results support the conclusion that the preorganization of the H463F TIL Trp complex, which is probably dominated by motion of the L-Trp indole moiety of the aldimine complex, contributes to quinonoid intermediate formation. Quinonoid intermediate formation may be gated by preorganization of the external aldimine, and thus, the enzyme is under a degree of dynamic control.

## CONCLUSIONS

The formation of the quinonoid intermediate from L-Trp by H463F TIL is influenced by pH, with pK<sub>a</sub> values of 7.54 and 8.14. These ionizations are not due to the active site base responsible for deprotonation but probably influence the reaction by changing the enzyme conformation. The rate constant for quinonoid intermediate formation is influenced by pressure, with an initial increase up to 100 MPa, followed by a decrease. These results are consistent with a significant preorganization of the external aldimine complex before deprotonation. The small and pressure-independent KIE seen with α-[<sup>2</sup>H]-L-Trp suggests that preorganization and/or conformational changes are rate-determining in quinonoid intermediate formation.

## AUTHOR INFORMATION

### Corresponding Author

\*Department of Chemistry, University of Georgia, Athens, GA 30602. Phone: (706) 542-1996. Fax: (706) 542-9454. E-mail: plp@uga.edu.

### Funding

S.H. is a United Kingdom Biotechnology and Biological Sciences Research Council (BBSRC) David Phillips Fellow.

### Notes

The authors declare no competing financial interest.

## ABBREVIATIONS

TIL, tryptophan indole-lyase or tryptophanase (EC 4.1.99.1); TPL, tyrosine phenol-lyase (EC 4.1.99.2); PLP, pyridoxal 5'-phosphate.

## REFERENCES

- (1) Snell, E. E. (1975) Tryptophanase: Structure, catalytic activities, and mechanism of action. *Adv. Enzymol. Relat. Areas Mol. Biol.* 42, 287–333.
- (2) Collet, A., Vilain, S., Cosette, P., Junter, G. A., Jouenne, T., Phillips, R. S., and Di Martino, P. (2007) Protein expression in *Escherichia coli* S17-1 biofilms: Impact of indole. *Antonie van Leeuwenhoek* 91, 71–85.
- (3) Di Martino, P., Merieau, A., Phillips, R., Orange, N., and Hulen, C. (2002) Isolation of an *Escherichia coli* strain mutant unable to form biofilm on polystyrene and to adhere to human pneumocyte cells: Involvement of tryptophanase. *Can. J. Microbiol.* 48, 132–137.
- (4) Di Martino, P., Fursy, R., Bret, L., Sundararaju, B., and Phillips, R. S. (2003) Indole can act as an extracellular signal to regulate biofilm formation in *Escherichia coli* and in other indole-producing bacteria. *Can. J. Microbiol.* 49, 443–449.

- (5) Lee, J., Maeda, T., Hong, S. H., and Wood, T. K. (2009) Reconfiguring the quorum-sensing regulator SdiA of *Escherichia coli* to control biofilm formation via indole and N-acylhomoserine lactones. *Appl. Environ. Microbiol.* 75, 1703–1716.
- (6) Chant, E. L., and Summers, D. K. (2007) Indole signalling contributes to the stable maintenance of *Escherichia coli* multicopy plasmids. *Mol. Microbiol.* 63, 35–43.
- (7) Anyanful, A., Dolan-Livengood, J. M., Lewis, T., Sheth, S., Dezaia, M. N., Sherman, M. A., Kalman, L. V., Benian, G. M., and Kalman, D. (2005) Paralysis and killing of *Caenorhabditis elegans* by enteropathogenic *Escherichia coli* requires the bacterial tryptophanase gene. *Mol. Microbiol.* 57, 988–1007.
- (8) Lee, H. H., Molla, M. N., Cantor, C. R., and Collins, J. J. (2010) Bacterial charity work leads to population-wide resistance. *Nature* 467, 82–85.
- (9) Phillips, R. S. (1989) The mechanism of tryptophan indole-lyase: Insights from pre-steady-state kinetics and substrate and solvent isotope effects. *J. Am. Chem. Soc.* 111, 727–730.
- (10) Phillips, R. S. (1991) The reaction of indole and benzimidazole with amino acid complexes of *E. coli* tryptophan indole-lyase: Detection of a new reaction intermediate. *Biochemistry* 30, 5927–5934.
- (11) Phillips, R. S., Sundararaju, B., and Faleev, N. G. (2000) Proton transfer and carbon-carbon bond cleavage in the elimination of indole catalyzed by *Escherichia coli* tryptophan indole-lyase. *J. Am. Chem. Soc.* 122, 1008–1114.
- (12) Phillips, R. S., Johnson, N., and Kamath, A. V. (2002) Formation *in vitro* of hybrid dimers of H463F and Y74F mutant *Escherichia coli* tryptophan indole-lyase rescues activity with L-tryptophan. *Biochemistry* 41, 4012–4019.
- (13) Phillips, R. S., and Holtermann, G. (2005) Differential effects of temperature and hydrostatic pressure on the formation of quinonoid intermediates from L-Trp and L-Met by H463F mutant *Escherichia coli* tryptophan indole-lyase. *Biochemistry* 44, 14289–14297.
- (14) Phillips, R. S., and Gollnick, P. D. (1989) Evidence that cysteine-298 is in the active site of tryptophan indole-lyase. *J. Biol. Chem.* 264, 10627–10632.
- (15) Bradford, M. M. (1976) A rapid and sensitive method for the quantitation of microgram quantities of protein utilizing the principle of protein-dye binding. *Anal. Biochem.* 72, 248–254.
- (16) Suelter, C. H., Wang, J., and Snell, E. E. (1976) Direct spectrophotometric assay of tryptophanase. *FEBS Lett.* 66, 230–232.
- (17) Kitamura, Y., and Itoh, T. (1987) Reaction volume of protonic ionization for buffering agents: Prediction of pressure dependence of pH and pOH. *J. Solution Chem.* 16, 715–725.
- (18) Frisch, M. J., Trucks, G. W., Schlegel, H. B., Scuseria, G. E., Robb, M. A., Cheeseman, J. R., Montgomery, J. A., Jr., Vreven, T., Kudin, K. N., Burant, J. C., et al. (2004) *Gaussian 03*, revision D, Gaussian, Inc., Wallingford, CT.
- (19) June, D. S., Suelter, C. H., and Dye, J. L. (1981) Kinetics of pH-dependent interconversion of tryptophanase spectral forms studied by scanning stopped-flow spectrophotometry. *Biochemistry* 20, 2707–2713.
- (20) Morino, Y., and Snell, E. E. (1967) The relation of spectral changes and tritium exchange reactions to the mechanism of tryptophanase-catalyzed reactions. *J. Biol. Chem.* 242, 2800–2809.
- (21) Sun, S., and Toney, M. D. (1999) Evidence for a two-base mechanism involving tyrosine-265 from arginine-219 mutants of alanine racemase. *Biochemistry* 38, 4058–4065.
- (22) Milić, D., Demidkina, T. V., Faleev, N. G., Phillips, R. S., Matković-Čalogović, D., and Antson, A. A. (2011) Crystallographic snapshots of tyrosine phenol-lyase show that substrate strain plays a role in C-C bond cleavage. *J. Am. Chem. Soc.* 133, 16468–16476.
- (23) Milić, D., Demidkina, T. V., Faleev, N. G., Matković-Čalogović, D., and Antson, A. A. (2008) Insights into the catalytic mechanism of tyrosine phenol-lyase from X-ray structures of quinonoid intermediates. *J. Biol. Chem.* 283, 29206–29214.
- (24) Isaacs, N. S., Javai, K., and Rannala, E. (1977) Pressure effects on proton tunnelling. *Nature* 268, 372–372.

(25) Hay, S., Sutcliffe, M. J., and Scrutton, N. S. (2007) Promoting motions in enzyme catalysis probed by pressure studies of kinetic isotope effects. *Proc. Natl. Acad. Sci. U.S.A.* 104, 507–512.

(26) Northrop, D. B. (2006) Unusual origins of isotope effects in enzyme-catalysed reactions. *Philos. Trans. R. Soc. London, Ser. B* 361, 1341–1349.

(27) Hay, S., and Scrutton, N. S. (2008) Incorporation of hydrostatic pressure into models of hydrogen tunneling highlights a role for pressure-modulated promoting vibrations. *Biochemistry* 47, 9880–9887.

(28) Pudney, C. R., Hay, S., Levy, C., Pang, J., Sutcliffe, M. J., Leys, D., and Scrutton, N. S. (2009) Evidence to support the hypothesis that promoting vibrations enhance the rate of an enzyme catalysed H-tunneling reaction. *J. Am. Chem. Soc.* 131, 17072–17073.

(29) Phillips, R. S., Miles, E. W., and Cohen, L. A. (1985) Differential inhibition of tryptophan synthase and of tryptophanase by the two diastereoisomers of 2,3-dihydro-L-tryptophan. Implications for the stereochemistry of the reaction intermediates. *J. Biol. Chem.* 260, 14665–14670.